

Facile synthesis of one-dimensional peapod-like Sb@C submicron-structures

The Faculty of Oregon State University has made this article openly available.
Please share how this access benefits you. Your story matters.

| | |
|---------------------|--|
| Citation | Luo, W., Lorget, S., Wang, B., Bommier, C., & Ji, X. (2014). Facile synthesis of one-dimensional peapod-like Sb@C submicron-structures. <i>Chemical Communications</i> , 50(41), 5435-5437. doi:10.1039/c4cc01326c |
| DOI | 10.1039/c4cc01326c |
| Publisher | Royal Society of Chemistry |
| Version | Accepted Manuscript |
| Terms of Use | http://cdss.library.oregonstate.edu/sa-termsofuse |

Cite this: DOI: 10.1039/c0xx00000x

www.rsc.org/xxxxxx

ARTICLE TYPE

Facile synthesis of one-dimensional peapod-like Sb@C submicron-structures

Wei Luo, Simon Lorgier, Bao Wang, Clement Bommier and Xiulei Ji*

Received (in XXX, XXX) Xth XXXXXXXXXX 20XX, Accepted Xth XXXXXXXXXX 20XX

DOI: 10.1039/b000000x

We demonstrate a novel synthetic route to fabricate a one-dimensional peapod-like Sb@C structure with disperse Sb submicron-particles encapsulated in carbon submicron-tubes. The synthetic route may well serve as a general methodology for fabricating carbon/metallic fine structures by thermally reducing their carbon-coated metal oxide composites.

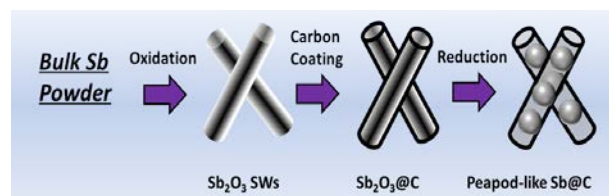
Submicron- and nano-structured materials have attracted great interest due to their superior physicochemical properties and wide applications.¹ Particularly, one-dimensional (1D) structures such as wires, tubes and fibers have attracted much attention.² Intense efforts have been made to design and prepare various 1D structures with innovative synthetic schemes.³ To date, most synthetic methodologies are based on template-assisted methods,⁴ self-assembly⁵ or chemical vapor deposition,⁶ which can be time-consuming or costly. Therefore, developing simple but efficient synthetic strategies to fabricate 1D structures still remains a great challenge.

Antimony (Sb) and its compounds have been extensively investigated due to their wide applications in lead-acid batteries, fire retardants, microelectronics and medicines.⁷ Recently, there has been increasing interest in employing Sb and its compounds as anodes for rechargeable lithium-ion or sodium-ion batteries.⁸ Owing to the alloying/dealloying reaction mechanism, these materials have higher theoretical capacities compared to the intercalation compounds (e.g., graphite and $\text{Li}_4\text{Ti}_5\text{O}_{12}$). However, like other alloying-type anodes (e.g., Si and Sn), these Sb-based anodes encounter a large volumetric change upon electrochemical cycling, which results in fast capacity fading. In order to overcome this issue, ongoing research efforts have focused on controlling the morphology into submicron- or nano-sizes^{8c,9} or coating with a carbon layer.¹⁰ Very recently, 1D Sb/C fibers have been fabricated by electrospinning a SbCl_3 /polyaniline (PAN) solution.¹¹ These 1D Sb/C fibers have shown a high capacity and enhanced cycle life.

In this communication, we present a novel synthetic route for the fabrication of 1D peapod-like Sb@C with disperse Sb submicron-particles encapsulated in carbon submicron-tubes by using bulk Sb powder as a precursor. As illustrated in Scheme 1, Sb_2O_3 submicron-wires (Sb_2O_3 SWs) are first prepared by direct air-oxidation of bulk Sb powder (~ 100 mesh) soaked in a mixture solution of a poly(vinyl pyrrolidone) (PVP) / ethylenediamine (EDA)/ H_2O , as reported previously.¹² Later, the as-prepared Sb_2O_3 SWs are coated with a layer of glucose-

derived carbon via a hydrothermal reaction, which gives an intermediate product (referred to as Sb_2O_3 @C). Then, a thermal reduction at 500 °C for 2 hrs under N_2/H_2 (5% in volume) converts Sb_2O_3 @C to 1D peapod-like structure with disperse Sb submicron-particles trapped in the “carbon submicron-tube pods”. Moreover, much void space appears in the carbon tubes due to the contraction from Sb_2O_3 SWs to Sb submicron-particles. We refer to the 1D peapod-like structure as Sb@C.

The crystalline structures of various materials are revealed by X-ray diffraction (XRD). As shown in Fig. 1a, bulk Sb powder exhibits a typical hexagonal phase of metallic Sb (JCPDS No. 35-0732). After the oxidation, the as-formed phase can be readily indexed to orthorhombic Sb_2O_3 (JCPDS No. 11-0689) (Fig. 1b). Moreover, the intensities of the (110) and (200) peaks in Sb_2O_3 SWs are greatly enhanced in comparison to the bulk counterpart, indicative of a strong orientation preference of wires along the [001] direction.¹² After the hydrothermal carbon coating, the crystalline structure of Sb_2O_3 @C remains the same (Fig. 1c). The final product of Sb@C exhibits the crystalline phase of hexagonal Sb, indicating the successful thermal reduction (Fig. 1d). Raman spectroscopy was further carried out (Fig. S1, see ESI†). Sb_2O_3 SWs exhibit typical Sb_2O_3 Raman shifts, displaying peaks at ~196, 225, 293, 380, 408, 455, and 503 cm^{-1} .^{12a} Sb@C displays similar Raman peaks as those from bulk Sb powder, corroborating the XRD results (Fig. 1). Moreover, Raman shifts from carbon (~1350 and 1590 cm^{-1}) suggest the existence of carbon in Sb@C. Furthermore, the I_D/I_G ratio of 0.91 suggests that the carbon layer is amorphous, which should be ascribed to the relatively-low thermal treatment temperature. The carbon content in the Sb@C is determined as ~ 25 wt% by thermogravimetric analysis (TGA), assuming the complete carbon combustion and formation of Sb_2O_4 at 800 °C (Fig. S2, see ESI†).^{11b}



Scheme 1 Schematic illustration for the formation of 1D peapod-like Sb@C submicro-structure by a simple oxidation-carbon coating-reduction route.

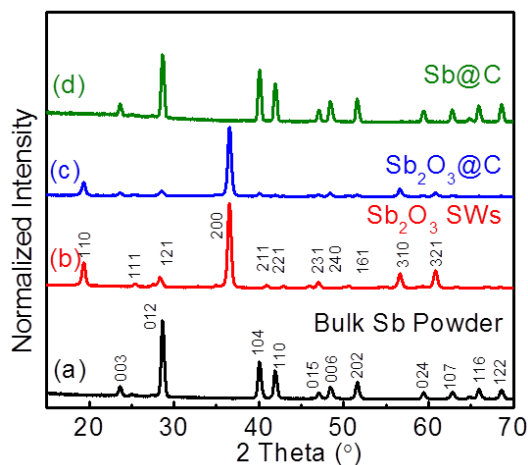


Fig. 1 XRD patterns of (a) bulk Sb powder, (b) Sb_2O_3 SWs, (c) $\text{Sb}_2\text{O}_3@C$ and (d) $\text{Sb}@C$.

Field-emission scanning electron microscopy (FESEM) images provide the morphological information of the materials. As shown in Fig. 2a and b, bulk Sb powder is well crystallized with particle sizes ranging from 5 to 40 μm . After oxidation, the as-formed Sb_2O_3 is composed of 1D submicron-wires with an average diameter of 800 nm and lengths up to tens of microns (Fig. 2c). When zoomed in, a smooth surface of Sb_2O_3 SWs is evident (Fig. 2d). The energy-dispersive X-ray (EDX) analysis confirms that the atomic ratio between Sb and O is $\sim 2/3$ in Sb_2O_3 SWs (Fig. S3, see ESI[†]). The growth mechanism of Sb_2O_3 SWs has been discussed by Deng et al. Sb is oxidized by dissolved oxygen in H_2O where EDA and PVP act as a catalyst and surface stabilizer, respectively.¹² After the hydrothermal carbon coating, the submicron-wire morphology is well maintained (Fig. S4, see ESI[†]). Compared to the EDX spectrum of Sb_2O_3 SWs, a new sharp peak of carbon appears after carbon coating (Fig. S3, see ESI[†]). After thermal treatment, the 1D shape is well maintained as well, and slight shrinkage in diameter is observed (Fig. 2e and f). Interestingly, the Sb_2O_3 wires encapsulated in carbon shells are converted to disperse Sb submicron-particles in the carbon submicron-tubes, exhibiting a peapod-like structure. Surprisingly, phase agglomeration does not occur when Sb_2O_3 is converted to Sb under thermal reduction. It is worth noting that the carbon coating plays a critical role for maintaining the 1D morphology of the composite. More FESEM images are provided in the supporting information to show the unique 1D peapod-like structure of $\text{Sb}@C$ (Fig. S5, see ESI[†]).

Fig. 3a shows a typical transmission electron microscope (TEM) image of an individual Sb_2O_3 submicron-wire. The corresponding high-resolution TEM (HRTEM) image taken on the edge is shown in Fig. 3b. The well-resolved lattice fringe with an inter-plane distance of ~ 1.25 nm is indexed to the (010) plane of the orthorhombic Sb_2O_3 .¹² The selected-area electron diffraction (SAED) pattern reveals the single-crystal nature of the Sb_2O_3 SWs along the [001] direction (Fig. 3c), which is consistent with the XRD results and previous reports.¹² The 1D peapod-like morphology of $\text{Sb}@C$ is further confirmed by TEM studies (Fig. S6, see ESI[†]). Zoomed-in TEM observation shows two disperse Sb submicron-particles are encapsulated in the

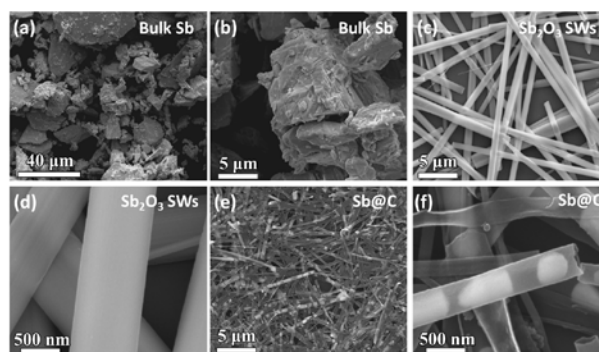


Fig. 2 Low and high-magnification FESEM images of bulk Sb powder (a, b), Sb_2O_3 NWs (c, d), and $\text{Sb}@C$ (e, f).

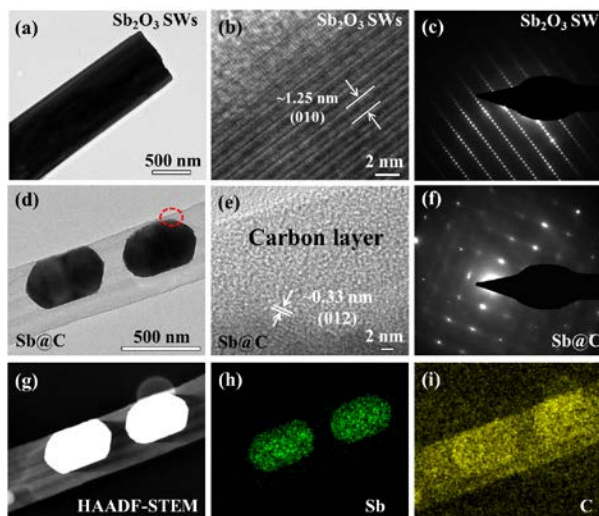


Fig. 3 TEM, HRTEM images and SAED patterns of Sb_2O_3 SWs (a, b, c) and $\text{Sb}@C$ (d, e, f). (g) HAADF-STEM and (h, i) corresponding elemental mapping images of $\text{Sb}@C$.

carbon submicron-tubes (in Fig. 3d). The HRTEM image taken on the red area marked in Fig. 3d further reveals the amorphous carbon structure for the carbon submicron-wires (Fig. 3e), which is typical for the sugar-derived carbon.¹³ Moreover, the lattice fringe with an inter-plane spacing of 0.33 nm from the Sb nanoparticle should be attributed to the (012) planes. The corresponding SAED pattern also suggests the single-crystal nature of Sb (Fig. 3f). Furthermore, Fig. 3g-i show the high angle annular dark field-scanning TEM (HAADF-STEM) and the corresponding EDX mapping images of $\text{Sb}@C$, confirming the peapod-like structure with a clear contrast.

Sodium-ion storage property of the as-prepared $\text{Sb}@C$ was studied by galvanostatic discharge-charge measurements using Na metal as the counter electrode and an electrolyte of 1.0 mol/L NaPF_6 in ethylene carbonate / diethyl carbonate (EC/DEC). Voltage plateaus are exhibited at about 0.5 V and 0.8 V in the discharge and charge curve, respectively (Fig. S7, see ESI[†]), suggesting a typical two-phase alloying reaction.⁹ The first discharge and charge capacity are ~ 335 and 230 mAh/g, respectively, based on the total mass of $\text{Sb}@C$ composites. The irreversible capacity in the first cycle may be attributed to the

formation of solid electrolyte interphase (SEI) on carbon. We recognize that the charge capacity of this composite is low. This can be due to the following issues. Firstly, the particle size of Sb phase is still relatively large, which may limit the utilization of Sb. Secondly, the electronic conductivity of the glucose-derived carbon as a coating layer is low due to the low carbonization temperature used.^{8d,8e,11} Further optimization is undergoing in our lab.

Conclusions

In summary, we have demonstrated a facile strategy for the fabrication of 1D peapod-like Sb@C submicron-structures with Sb submicron-particles and large void space encapsulated in the carbon submicron-tubes. Considering the low cost of the starting materials and simple synthetic process, we believe our method may shed some light on a scalable fabrication of Sb-based materials and other peapod-like structures.

Acknowledgements

The authors acknowledge the financial support from Advanced Research Projects Agency-Energy (ARPA-E), Department of Energy of the United States, Award number: DE-AR0000297TDD. We are thankful to Ms. Teresa Sawyer and Dr. Peter Eschbach for the SEM and TEM measurements in OSU EM Facility, funded by National Science Foundation via the Major Research Instrumentation Program under Grant No. 1040588, Murdock Charitable Trust and the Oregon Nanoscience and Microntechnologies Institute. We appreciate the help from Professor Chih-Hung Chang and Mr. Changqing Pan for Raman analysis.

Notes and references

Department of Chemistry, Oregon State University, Corvallis, OR 97331-4003, USA. Tel: 001 541-737-6798; E-mail: david.ji@oregonstate.edu

† Electronic Supplementary Information (ESI) available: Experimental details and additional data. See DOI: 10.1039/b000000x/

- (a) P. G. Bruce, B. Scrosati and J. M. Tarascon, *Angew. Chem. Int. Ed.*, 2008, **47**, 2930-2946; (b) X. W. Lou, L. A. Archer and Z. C. Yang, *Adv. Mater.*, 2008, **20**, 3987-4019; (c) K. T. Lee and J. Cho, *Nano Today*, 2011, **6**, 28-41.
- (a) Y. Xia, P. Yang, Y. Sun, Y. Wu, B. Mayers, B. Gates, Y. Yin, F. Kim and H. Yan, *Adv. Mater.*, 2003, **15**, 353-389; (b) Z. L. Wang, *Adv. Mater.*, 2003, **15**, 432-436; (c) Z. Tang and N. A. Kotov, *Adv. Mater.*, 2005, **17**, 951-962; (d) Z. W. Pan, Z. R. Dai and Z. L. Wang, *Science*, 2001, **291**, 1947-1949; (e) Z. L. Wang and J. Song, *Science*, 2006, **312**, 242-246.
- (a) H. Q. Yan, R. R. He, J. Pham and P. D. Yang, *Adv. Mater.*, 2003, **15**, 402-405; (b) X. W. Lou, D. Deng, J. Y. Lee, J. Feng and L. A. Archer, *Adv. Mater.*, 2008, **20**, 258-262; (c) D. Li and Y. Xia, *Adv. Mater.*, 2004, **16**, 1151-1170; (d) X. L. Hu and J. C. Yu, *Chem. Mater.*, 2008, **20**, 6743-6749; (e) J. He, B. Yu, M. J. Hourwitz, Y. Liu, M. T. Perez, J. Yang and Z. Nie, *Angew. Chem. Int. Ed.*, 2012, **51**, 3628-3633.
- (a) S. J. Hurst, E. K. Payne, L. Qin and C. A. Mirkin, *Angew. Chem. Int. Ed.*, 2006, **45**, 2672-2692; (b) M. Kogiso, K. Yoshida, K. Yase and T. Shimizu, *Chem. Commun.*, 2002, 2492-2493.
- (a) Z. Gu, Y. Ma, W. Yang, G. Zhang and J. Yao, *Chem. Commun.*, 2005, 3597-3599; (b) L. Zang, Y. Che and J. S. Moore, *Acc. Chem. Res.*, 2008, **41**, 1596-1608; (c) J. He, Y. Liu, T. Babu, Z. Wei and Z. Nie, *J. Am. Chem. Soc.*, 2012, **134**, 11342-11345; (d) Z. Nie, A. Petukhova and E. Kumacheva, *Nat. Nanotechnol.*, 2010, **5**, 15-25.

- (a) Y. Cui, Q. Wei, H. Park and C. M. Lieber, *Science*, 2001, **293**, 1289-1292; (b) Y. Wu, R. Fan and P. Yang, *Nano Lett.*, 2002, **2**, 83-86.
- (a) B. Poudel, Q. Hao, Y. Ma, Y. Lan, A. Minnich, B. Yu, X. Yan, D. Wang, A. Muto, D. Vashaee, X. Chen, J. Liu, M. S. Dresselhaus, G. Chen and Z. Ren, *Science*, 2008, **320**, 634-638; (b) W. R. Osório, D. M. Rosa, L. C. Peixoto and A. Garcia, *J. Power Sources* 2011, **196**, 6567-6572; (c) M. Zanetti, G. Camino, D. Canavese, A. B. Morgan, F. J. Lamelas and C. A. Wilkie, *Chem. Mater.*, 2001, **14**, 189-193; (d) R. Ge and H. Sun, *Acc. Chem. Res.*, 2007, **40**, 267-274.
- (a) H. Kim and J. Cho, *Chem. Mater.*, 2008, **20**, 1679-1681; (b) L. M. L. Fransson, J. T. Vaughey, R. Benedek, K. Edström, J. O. Thomas and M. M. Thackeray, *Electrochem. Commun.*, 2001, **3**, 317-323; (c) H. Li, X. Huang and L. Chen, *Solid State Ionics*, 1999, **123**, 189-197; (d) L. Xiao, Y. Cao, J. Xiao, W. Wang, L. Kovarik, Z. Nie and J. Liu, *Chem. Commun.*, 2012, **48**, 3321-3323; (e) J. Qian, Y. Chen, L. Wu, Y. Cao, X. Ai and H. Yang, *Chem. Commun.*, 2012, **48**, 7070-7072.
- A. Darwiche, C. Marino, M. T. Sougrati, B. Fraisse, L. Stievano and L. Monconduit, *J. Am. Chem. Soc.*, 2012, **134**, 20805-20811.
- (a) Y. Zhang, J. Xie, T. Zhu, G. Cao, X. Zhao and S. Zhang, *J. Power Sources*, 2014, **247**, 204-212; (b) H. Li, Q. Wang, L. Shi, L. Chen and X. Huang, *Chem. Mater.*, 2001, **14**, 103-108; (c) S. H. Lee, M. Mathews, H. Toghiani, D. O. Wipf and J. C. U. Pittman, *Chem. Mater.*, 2009, **21**, 2306-2314.
- (a) Y. Zhu, X. Han, Y. Xu, Y. Liu, S. Zheng, K. Xu, L. Hu and C. Wang, *ACS Nano*, 2013, **7**, 6378-6386; (b) L. Wu, X. Hu, J. Qian, F. Pei, F. Wu, R. Mao, X. Ai, H. Yang and Y. Cao, *Energy Environ. Sci.*, 2014, **7**, 323-328.
- (a) Z. Deng, F. Tang, D. Chen, X. Meng, L. Cao and B. Zou, *J. Phys. Chem. B*, 2006, **110**, 18225-18230; (b) Z. Deng, D. Chen, F. Tang, X. Meng, J. Ren and L. Zhang, *J. Phys. Chem. C*, 2007, **111**, 5325-5330.
- (a) X. W. Lou, D. Deng, J. Y. Lee and L. A. Archer, *Chem. Mater.*, 2008, **20**, 6562-6566; (b) X. W. Lou, C. M. Li and L. A. Archer, *Adv. Mater.*, 2009, **21**, 2536-2539.